Composite Structures 104 (2013) 215–229

Contents lists available at SciVerse ScienceDirect

Composite Structures

journal homepage: www.elsevier.com/locate/compstruct

# Multi-resolution finite element models for simulation of the ballistic impact on non-crimped composite fabric packages

Rimantas Barauskas [a,*], Ausra Abraitiene [b]

[a] Department of System Analysis, Kaunas University of Technology, Studentu 50, LT – 51368 Kaunas, Lithuania
[b] Lithuanian Textile Institute, Demokratu 53, LT – 48485 Kaunas, Lithuania

ARTICLE INFO

*Article history:*
Available online 25 April 2013

*Keywords:*
Non-crimped composite fabric
Ballistic interaction
Failure
Finite elements
Multi-scale models
LS-DYNA

ABSTRACT

A multi-scale finite element model for the simulation of medium velocity ballistic impact on non-crimped laminated composite fabric packages has been developed in LS-DYNA. The targets are soft fabric structures of non-crimped fibre plies bonded together by polymeric filling. The model of each fibre ply is divided into farther and nearer to impact zones. The farther zone is a macro-level model of orthotropic homogeneous membrane, and the nearer zone is a mezzo level structure composed of narrow aramid strips and polymeric gaskets. Shell elements are used for all the structural components of the fibre ply. The macro-level models employs the material properties determined on the base of the finite element analysis of the micro-cube representing a small fragment of the fibre bundle. At mezzo level the material properties are modified by using a mezzo-cube, which represents the narrow strip and gasket together. The convergence of the narrow strips model is demonstrated. Simultaneously with the combined macro-mezzo level model of a ply two different macro-level models are investigated. Good agreement among the results provided by different models has been established by proper adjustment of erosion strain parameter on the base of reference results obtained at mezzo level.



## 1. Introduction

The goal of this research is to develop models and software tools for simulation of ballistic impact of a deformable bullet against non-crimped laminated fabric multilayers. The fabric multilayers are employed as structural parts of lightweight body armour, which nowadays is worn everyday by the army, police and used in other dangerous services. The principle of action of the packages is based on the transformation of kinetic energy of the bullet into elastic–plastic strain energy dissipated within the layers of the package and within the deformed bullet itself.

The ballistic protection packages are subjected to ballistic tests. A package is attached to a plasticine block, which imitates the mechanical resistance of human body, and hit by a bullet of certain type, mass and velocity. The package should not be shot through and the depth of the pit in the plasticine should not exceed certain critical value. Therefore simulation of the ballistic test is important practically as it enables to predict the ballistic resistance of packages of different compositions.

Differently from widely used stiff composite structures, the investigated objects are soft fabric structures made of thin flexible non-crimped multi-fibre composite layers. They are different also from widely used flexible woven fabric structures. A sheet of non-woven fabrics may be composed of 4 or more orthogonal non-crimped fibre plies.

The difficulties in modelling and simulation occur due to the loose binding of fibres within the fabric, the absence of stiff composite matrices and low saturation of inter-fibre spaces by the polymeric pitch. During the impact essential changes of geometrical forms and local patterns of yarns and fibres in the vicinity of the interaction point occur long before the final failure. The macro-level models based on homogeneous membranes very often fail to provide satisfactory results. Large strains, structural changes and partial failure prevent from obtaining unique and adequate constitutive models within the full deformation range.

The multi-domain, embedded, parallel, serial and other multi-scale modelling approaches are known [1,2]. The homogenization approaches are directly applicable to the bridging of micro and macro-scale models of stiff composites, [3,4]. The homogenization approach has been applied to partially damaged micro-fragments. The linear material behaviour model has been supplemented by degradation relationships of stiffness coefficients due to breaking of certain number of yarns. However, the pure homogenization approaches are applicable if the stresses and strains up to failure point have to be determined. If the simulation has to be continued after the complete failure and disintegration of certain parts of the

* Corresponding author.
*E-mail addresses:* rimantas.barauskas@ktu.lt (R. Barauskas), lti@lti.lt (A. Abraitiene).

0263-8223/$ - see front matter © 2013 Elsevier Ltd. All rights reserved.
http://dx.doi.org/10.1016/j.compstruct.2013.04.014

structure, other approaches are necessary. In this study we concentrate on combined models based on homogenization and on development of appropriate architecture of the mezzo level model.

The inherent feature of mezzo level models is the representation of the most important formations of the modelled object by including them directly into the patterns of the finite element structure. Many publications have been devoted to the development of mezzo level woven structures models. Early approach [5] presented an elastically supported fragment of woven patch, presented as geometrical imitation of woven patterns by chains of shell elements subjected to contact interactions with each other. The material model of the shell elements was elastic–plastic isotropic, where the failure of the elements was determined by the value of effective strain. The modelling idea was extended in [6], where near and far zones with respect to the impact point have been distinguished. The near zone employed the woven patch model, whereas the far zone was presented by the continuous orthotropic membrane model. The material properties values of the membrane had been found, which ensure the seamless propagation of impact waves through the interface between and through the two zones.

Other architectures of finite element models of woven structures have been employed in [7–14]. In [7] the impact on woven fabric has been modelled by using a discrete spring structure, where the properties of springs have been obtained as a result of experimental investigations. In [8], LSDYNA material N19 has been applied for modelling the fabric, which has been hit by the spherical projectile. The analysis included only one layer of fabric. In [9] a woven patch modelled by 3D solid elements was introduced. The work was devoted to analysis of influence of friction on the interaction properties between the patch and the rigid sphere. [10] presented a multi-scale structure and iterative scheme for the modelling the dynamic interaction against the fabric, where simulations were carried out at the fibril level and at the interacting yarn structure level. The yarns were presented as rod elements. In [11] two zones of fabric have been modelled by applying different woven structures. The near-to-impact zone was presented as a woven structure of 3D solid elements, and the farther woven zone employed the shell elements. In [12] the same authors supplied the third 'global' zone to the earlier model, which was modelled by using the homogeneous membrane. The overall model of the impact on a woven fabric implemented completely at micro-level by using digital element technique has been described in [13].

Laminated textile fabrics consist of woven or non-crimped laminated composite fabric (NCLCF) structure bonded together by polymeric thermoplastic resin and polyethylene films over their external surfaces. Application of NCLCF in ballistic protection packages offers wide opportunities because of lesser costs and ability to resist the penetration of humidity, which may substantially decrease the ballistic strength of the structure. Another advantage is that in NCLCF the aramide filaments are not weekend by crimping, which is inherent in woven structures.

In this work finite element models of NCLCF laminate are proposed at mezzo mechanical level, which presents the components of NCLCF as a structure of orthotropic shell elements. The ballistic response of the fabric against deformable 6 mm bullets has been investigated.

The architecture of the model used in this work reflects the real structure of the NCLCF. Models have been generated at micro-mechanical (which present a small micro-cube of 3D filament structure), mezzo-mechanical (which present yarns bundles as smallest structural units) and macro-mechanical (which present NCLCF as a continuous orthotropic membrane) level. Numerical experiments made on micro-cubes enabled to establish average material properties used in mezzo-mechanical models. Mezzo-mechanical models in their turn serve for verification of macro-mechanical ones.

## 2. Combined model of non-crimped laminated composite fabric layer

Basic structural components of the NCLCF are unidirectional aramid fibre plies, from which the NCLCF sheets are formed, Fig. 1a. Most often 4 orthogonally oriented plies per sheet are bonded together by means of the polymer filling, which partially saturates the inter-fibre spaces of the NCLCF. The fastening is rather weak and fails very soon as impact loads are applied. Therefore during the impact we treat the plies as separate interacting parts.

By taking into account the nature of the interaction the FE model of a ply is considered as two-zone structure, Fig. 1b. The farther from the impact point zone is presented as homogeneous orthotropic membrane, the failure and structural change of which during the impact interaction is not expected. The nearer to impact zone, in which the failure takes place, is presented as a narrow strips structure. Each strip represents a bundle of fibres. Though a ply is generally considered as a uniform layer of parallel fibres, in reality it is made of slightly twisted fibres bundles situated in parallel to each other. This is determined mainly by technological considerations. The width $D = 1$ mm of the bundle within the structure and the thickness $\sim$0.1 mm may be regarded as realistic values. In our model the width of strip equals the shell element size. There is a narrow elastic–plastic gasket junction (width $d$) in between each two narrow strips, Fig. 2a. Such constitution of the model guarantees that the failure of the ply starts as the mutual separation of adjacent fibres bundles. Fig. 2a provides an illustration of orthotropic homogenized model of the fibres ply. Materials constants of the farther zone of the model are established on the base on the FE

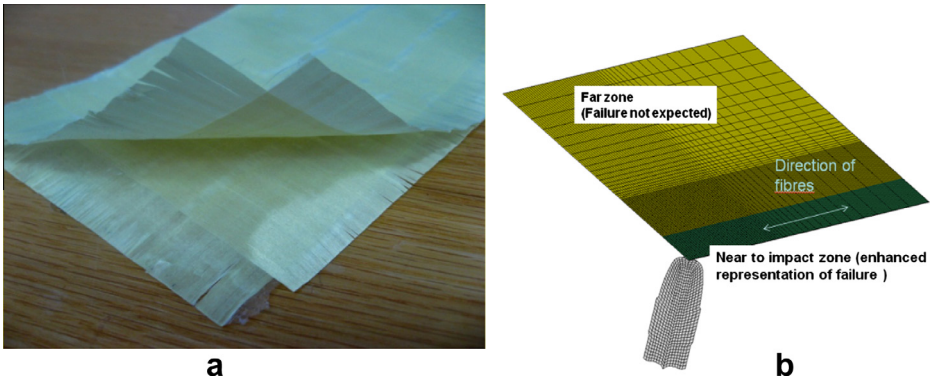


**Fig. 1.** The structure of the 4-plies sheet of NCLCF (a) and the geometry of the finite element model of the single ply (b).

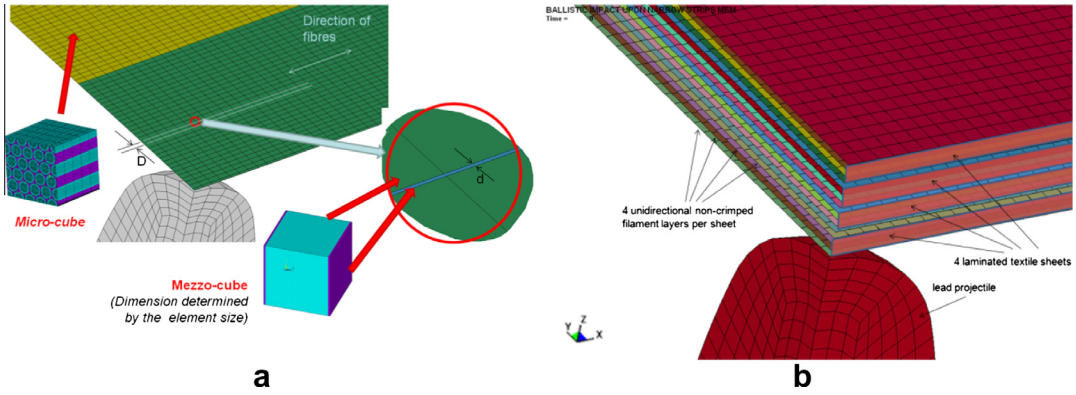


**Fig. 2.** The schemes of computational models of the fibres ply (a) and of the NCLCF package (b).

analysis of the micro-cube. The materials constants of the nearer to impact zone are adjusted on the base of the analysis of mezzo-cube, as will be explained later.

From the mathematical point of view, the width of a finite strip is not strictly prescribed. The width of the strip must ensure the convergence of the model, which is investigated on the base of comparison of dynamic responses of the structure obtained by using different widths of strips. Practically, the applicable width depends on the speed and energy of dynamic loading and on geometrical and structural properties of the ballistic impact zone. The model of the farther zone is referred to as *the macro-level model*. It presents the structure of unidirectional fibres held-up together by means of the soft polymeric filling as the homogeneous orthotropic membrane. The model of the near zone can be referred to as *the mezzo-level model*. It takes into account certain additional geometrical properties, which specify the structure. However, it is not a micro-level model as the narrow strip elaborates the structure to the level of fibres bundles and not to the level of individual fibres.

The maximum allowable time integration step in numerical equation solving is governed by the well-known Courant–Friedrichs–Lewy condition, which states that, given a space discretization, a time step bigger than some computable quantity should not be taken. As an example, the central difference time integration scheme requires to apply the time integration step not bigger than approximately half of the time period during which the longitudinal wave propagates the distance equal to the smallest linear measurement of an element. As the width $d$ of gasket elements is very small, extremely small time integration steps during the explicit dynamic analysis may severely reduce the computational efficiency. Fortunately, the difficulty is easily avoided. First, the stiffness module of the polymeric gasket is much less than the stiffness module of the aramid and the wave propagation speed within the polymer is low. Second, artificial mass scaling may be employed. The mass scaling means that the mass density value of the gasket is taken several times bigger than it is in reality. The result is the reduction of the wave propagation speed and subsequently the bigger allowable value of the time integration step. Artificial increase of the mass density of the gasket material inevitably introduces certain errors of the simulation results. Therefore in this problem mass scaling can be used only if the total mass of the structure is not increased significantly.

Finally, the overall FE model of the NCLCF package is composed of the FE models of fibres plies situated one upon another. Contact interaction properties of each pair of adjacent plies determine whether the plies belong to the same sheet of the NCLCF or to two different adjacent sheets, Fig. 2b. The tie-break contact interaction is employed between each pair of adjacent plies belonging to the same sheet. As the normal or tangential limiting contact stresses are exceeded, the tie bonds keeping both plies together are eliminated. Only unilateral mechanical contact with friction is to be considered during the remaining time period of simulation. The contact interactions between the top ply of one and the bottom ply of the other sheet are governed by unilateral mechanical contact with friction conditions all the simulation time. The projectile (bullet) is always in contact condition with all plies of the model all the simulation time.

## 3. Material models

### 3.1. Homogenized orthotropic stiffness constants

The modelling scheme is based on the serial employment of models composed at different length scales. The micromechanical model of a fragment of the parallel fibre ply filled in by the polymer is presented in Fig. 3a. The homogenized mechanical stiffness constants of the structure are obtained by performing the FE analysis of the mechanical behaviour of the micro-cube, Fig. 3b.

Pure strain components of the micro-cube are created by prescribing the necessary displacements of the sides of the micro-cube. The micro-level finite element model is employed for computing stresses within the micro-cube. Example vector plots of displacements, which create unity strains $\varepsilon_x$ and $\gamma_{yz}$ of the micro-cube and contours of calculated stresses are presented in Fig. 4. The average values of stresses over the micro-cube can be used for obtaining the stiffness tensor (in Voigt's notation) by means of the relation

$$[\mathbf{C}] = \begin{bmatrix} (\sigma_x)_1 & (\sigma_x)_2 & (\sigma_x)_3 & (\sigma_x)_4 & (\sigma_x)_5 & (\sigma_x)_6 \\ (\sigma_y)_1 & (\sigma_y)_2 & (\sigma_y)_3 & (\sigma_y)_4 & (\sigma_y)_5 & (\sigma_y)_6 \\ (\sigma_z)_1 & (\sigma_z)_2 & (\sigma_z)_3 & (\sigma_z)_4 & (\sigma_z)_5 & (\sigma_z)_6 \\ (\tau_{yz})_1 & (\tau_{yz})_2 & (\tau_{yz})_3 & (\tau_{yz})_4 & (\tau_{yz})_5 & (\tau_{yz})_6 \\ (\tau_{xz})_1 & (\tau_{xz})_2 & (\tau_{xz})_3 & (\tau_{xz})_4 & (\tau_{xz})_5 & (\tau_{xz})_6 \\ (\tau_{xy})_1 & (\tau_{xy})_2 & (\tau_{xy})_3 & (\tau_{xy})_4 & (\tau_{xy})_5 & (\tau_{xy})_6 \end{bmatrix} \begin{bmatrix} (\varepsilon_x)_1 & & & & & \\ & (\varepsilon_y)_2 & & & & \\ & & (\varepsilon_z)_3 & & & \\ & & & (\gamma_{yz})_4 & & \\ & & & & (\gamma_{yz})_4 & \\ & & & & & (\gamma_{yz})_4 \end{bmatrix}^{-1}, \quad (1)$$

where the lower numerical indices are loading cases numbers, $\sigma$, $\tau$ are longitudinal and shear stresses, $\varepsilon$ and $\gamma$ are longitudinal and shear strains.

The obtained linear expression of the stiffness tensor is valid only for small strains. For finite strains relations, the geometrically non-linear FE analysis of the micro-cube is performed. The results of the analysis are obtained in terms of true stresses, which are related with true (Hencky) strains by means of the stiffness tensor. In the geometrically non-linear case the displacements of the sides of the micro-cube have to be determined, which ensure certain chosen values of the components of true strains. The true strains values obtained from non-linear FE analysis and substituted to (1) provide the components of stiffness tensor, which is valid for the chosen values of strains. Non-linear analysis of the micro-cube should be performed at different values of strains and strain dependent values of the stiffness tensor are obtained.

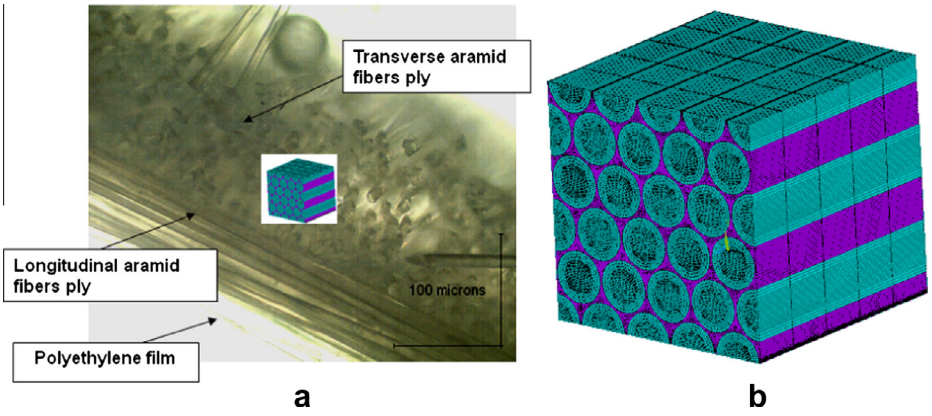


**Fig. 3.** The photo of the micro-structure of the unidirectional fibre ply (a) and the FE model of the micro-cube (b).

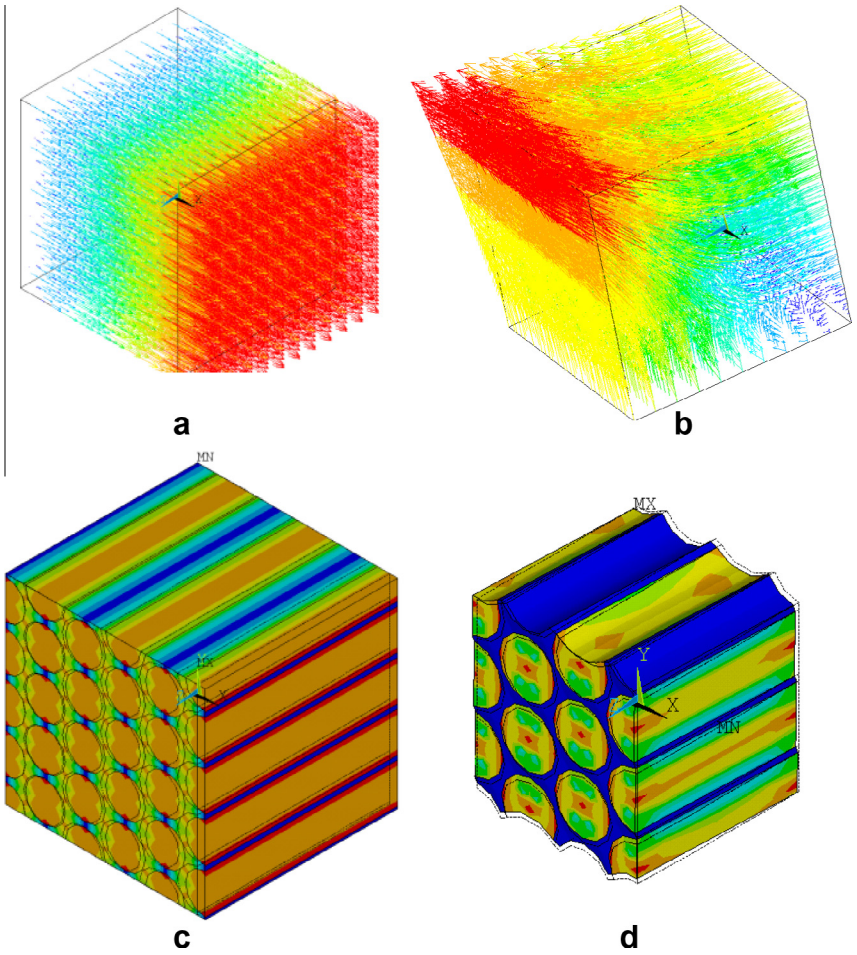


**Fig. 4.** Artificially created displacements providing pure strain components $\varepsilon_x$ (a) and $\gamma_{yz}$ (b) of the micro-cube and calculated stresses (c, d).

The displacements of sides of the micro-cube, which ensure the prescribed values of true strains, are calculated as follows. We present the explanation in 2D case.

The true strain tensor reads as

$$[\boldsymbol{\varepsilon}^H] = \ln([\mathbf{I}] + 2[\boldsymbol{\varepsilon}^G]); \tag{2}$$

where $[\mathbf{I}]$ is the unity matrix, $[\boldsymbol{\varepsilon}^G] = \begin{bmatrix} s + \frac{1}{2}(s)^2 + \frac{1}{2}(g)^2 & g + gs \\ g + gs & s\frac{1}{2}g^2 + \frac{1}{2}(s)^2 \end{bmatrix}$ is the Green's strain tensor; $g = \tan\gamma$; $\frac{\partial u}{\partial Y} = \frac{\partial v}{\partial X} = g; \frac{\partial u}{\partial X} = \frac{\partial v}{\partial Y} = s$; $g$ is shearing angle of the micro-cube; and $u$, $v$ is the displacements along $Ox$ and $Oy$ axes.

Pure longitudinal strains are obtained by taking $g = 0$, and pure shear strains are obtained by taking $s = \frac{-2\pm\sqrt{4-4g^2}}{2} = -1 \pm \sqrt{1-g^2}$.

Displacements $u_A$, $v_A$ of any point $A(x_A, y_A)$ on the surface of the micro-cube are calculated as

$$\begin{cases} u_A = x_A \frac{\partial u}{\partial x} + y_A \frac{\partial u}{\partial y}; \\ v_A = x_A \frac{\partial v}{\partial x} + y_A \frac{\partial v}{\partial y} \end{cases} \tag{3}$$

Aramid fibres and low density polyethylene as polymer filling were used in the FE model of the micro-cube. The numerical values employed in the sample calculations of this study are listed in Table 1. Practically, we used average values of the stiffness tensor obtained over strain range [0,1].

After substituting the values of calculated stresses averaged over the volume of the micro-cube into (1), the homogenized stiffness constants of orthotropic homogeneous material are obtained as listed in Table 2.

### 3.2. Constants of mezzo level model

The fibre ply of the mezzo level model is represented by two different material models. In the farther zone the orthotropic homogeneous membrane model is used, where two different stiffness module values in longitudinal and transverse directions are employed. In the nearer zone the same orthotropic material properties are exhibited by the combination of the narrow strip and gasket elements. Both models are implemented in LS-DYNA finite element software. The Belytschko–Lin–Tsay shell elements are based on a combined co-rotational and rate-of-deformation formulation, which make the element computationally efficient. The co-rotational formulation avoids the complexities of non-linear mechanics by embedding the coordinate system in the elements. The choice of rate-of-deformation in the formulation facilitates the constitutive evaluation, since the conjugate stress is the physical Cauchy stress [14]. Arbitrary number of through-thickness integration points can be chosen. The element may represent multi-layered materials, where individual orientation of the orthotropic axes may be indicated for each layer. One through-thickness integration point is necessary for each layer. Such elements enable to create various architectures of the models of NCLCF sheets and packages, as demonstrated further in this text.

The laminated composite fabric material model (material N58 in LS-DYNA) is used in this work. This orthotropic material intended to be used for modelling of composite materials with unidirectional layers, complete laminates, and woven fabrics. The elastic properties of the orthotropic material are characterized by its Young's moduli in two directions, Poisson's coefficient and shear moduli in three coordinate planes. The linear part of the shear strain–stress relationship is followed by the slightly non-linear strain–stress relationship, whereas the longitudinal strain–stress relationship remains linearly elastic until the failure point is reached. The failure mechanisms provided by the material model are discussed in detail further in this chapter.

**Table 2**
Mechanical constants of the fibres and filling.

| | |
|---|---|
| *Aramide* | |
| Young's modulus | 9e+010 N/m$^2$ |
| Poisson ratio | 0.3 |
| Mass density | 1400 kg/m$^3$ |
| Failure strain | 0.04 |
| *Low density polyethylene* | |
| Young's modulus | 3e+08 N/m$^2$ |
| Poisson ratio | 0.2 |
| Yield stress | 2e+07 kg/m$^2$ |
| Mass density | 920 kg/m$^3$ |
| Failure strain | 5 |
| *Lead* | |
| Young's modulus | 1.7e+10 N/m$^2$ |
| Poisson ratio | 0.4 |
| Yield stress | 8e+06 kg/m$^2$ |
| Hardening modulus | 1.5e7 kg/m$^2$ |
| Mass density | 11,270 kg/m$^3$ |
| Kinematic hardening parameter beta | 0.1–0.2 |
| Symonds–Cowper model parameter $C$ | 600 |
| Symonds–Cowper model parameter $p$ | 3 |

The direct experimental determination of numerous constants governing the non-linear behaviour and dynamic failure of the fabric made of freely bonded orthogonal thin fibre plies structures is complicated, therefore certain calculations and assumptions are necessary.

The homogenized orthotropic stiffness constants are determined by employing the results of the stiffness analysis of the micro-cube (see Section 3.1). The appropriate constants of the stiffness tensor are used as Young's moduli, Poisson's ratio and shear moduli of the material, Table 1. Direction $a$ is along the fibres, $b$ is the transverse direction on the plane of the ply, and $c$ is the transverse direction perpendicular to the plane of the ply.

The non-linear behaviour and failure properties of the material model are determined by several constants, the physical meaning of which is illustrated in Fig. 5. Two different kinds of failure conditions are used in order to present the failure of the laminated composite fabric material.

**Table 1**
Mechanical constants of the homogeneous model of unidirectional ply.

| | | Orthotropic homogeneous | Narrow strips |
|---|---|---|---|
| *Elastic constants and mass density* | | | |
| Ea | Longitudinal Young's modulus | 7.9e+10 N/m$^2$ | 7.91e+010 N/m$^2$ |
| Eb | Transverse Young's modulus | 7.5e+9 N/m$^2$ | 7.68e+009 N/m$^2$ |
| Prab | Major Poisson ratio | 0.05 | |
| Gab | Shear moduli corresponding to planes ab, bc, ca | 6.3e+9 N/m$^2$ | 6.63e+009 N/m$^2$ |
| Gbc | | 1.98e+9 N/m$^2$ | 2.01e+009 N/m$^2$ |
| Gca | Mass density | 6.3e+9 N/m$^2$ | 6.63e+009 N/m$^2$ |
| rho | | 1298 kg/m$^3$ | 1298.4 kg/m$^3$ |
| *Non-linear and failure constants* | | | |
| Xc, Xt | Limit longitudinal stress | 3.16e+9 N/m$^2$ | |
| Yc, Yt | Limit transverse stress | 3.19e+8 N/m$^2$ | |
| E11C, E11T | Limit longitudinal strain | 0.04 | |
| E22C, E22T | Limit transverse strain | 0.0425 | |
| SLIMTi | Tensile stiffness reduction coefficient | 0.01 | |
| SLIMCi | Compressive stiffness reduction coefficient | 1 | |
| TAU1 | Constants of shear strain–stress curve | 2e+7 N/m$^2$ | |
| GAMMA1 | | 0.0008 | |
| SC | Limit shear stress | 2.2e+7 N/m$^2$ | |
| GMS | Limit shear strain | 0.0211 | |
| ERODS | Effective erosion strain | 1.2 | 2 |

The first kind of failure conditions is described by essential reduction of the stress value in each characteristic direction within the element. This is valid for all strain–stress components. Individual values for tension and compression may be indicated. The pairs of strain–stress values (E11T, XT) and (E22T, YT) should be treated as points on the tensile strain–stress curves, at which failure of the material in this particular direction is expected. Pairs (E11C, XC) and (E22C, YC) are used in order to indicate the compressive failure points. The failure of the element means the reduction of the stiffness of the element rather than the deletion of the element from the structure. The stiffness reduction is performed by limiting the stress values by using tensile stress reduction coefficients SLIMT1, SLIMT2, compressive stress reduction coefficients SLIMC1, SLIMC2 and shear stress reduction coefficient SLIMS, as shown in Fig. 5. For example, if the tensile failure point is reached along direction *X*, in further calculations the longitudinal stress of the element along direction *X* is always equal to SLIMT1∗XC irrespective of the strain value. This means that the element continues to deform in all directions, however, further it exhibits the elastic strain–stress behaviour only along direction *Y* and in shearing. Even if the stiffness of the element is reduced in all directions, the element still remains in the structure and continues to deform. Fully reduced-stress elements are not able to exhibit any marked resistance to deformation and therefore their strains may become very large. In many cases such mathematical description of the failure mechanism appears as more adequate to the reality than the immediate deletion of overstrained elements. In reality multi-fibre plies cannot break immediately in any direction because of slightly different lengths and directions of individual fibres within the ply. In this study tensile stress reduction coefficient values SLIMT1, SLIMT2 were used as 0.01, and the corresponding compressive coefficient values SLIMC1, SLIMC2 equal to 1. In ballistic penetration problems we assume that in the case of compression the damaged material does not disappear and still exhibits resistance to further compression. The model of linear elastic material behaviour up to the failure point suits very well for aramid fibres. They remain nearly elastic up to the tensile strain failure limit ~0.04, at which they break. In case of medium velocity ballistic interaction problems this strain limit may be taken as slightly higher, however, in this numerical study we suppose that the strain limit for aramid is 0.04 irrespective of the strain rate. The values of limiting longitudinal strains and stresses indicated in Table 1 are based on this assumption.

The second failure condition ERODS is used in order to delete the overstrained elements from the model. Mathematically ERODS means the effective strain of the element, which combines all the components of the strain tensor. Therefore this failure parameter may seem to be at certain discrepancy with the element stresses reduction-based failure mechanism along individual directions. However, we demonstrate that appropriate usage of the parameter may provide additional capabilities, which enable to achieve realistic behaviour of the structure at very large overall deformations.

ERODS value should ensure that the element is not deleted until the element stresses are not reduced in all the directions (*X*, *Y* and shearing). The danger of premature deletion of the element may be explained as follows. For example, the fibre ply is subdued to very large straining in the direction perpendicular to fibres. Though physically the element of the ply may retain the full strength in the direction of fibres, it may be prematurely deleted because the contribution of the strain component perpendicular to fibres is enough to exceed the effective strain value ERODS. Therefore the ERODS value has to be adjusted carefully and in strict accordance with specific features of the investigated problem.

On the other hand, ERODS value should ensure that the model is not polluted by overstrained elements. During the explicit simulation of the impact interaction the elements the stiffness of which is reduced, still remain in the structure and take part in contact interactions. Because of the reduced stiffness the failed elements eventually acquire unrealistic geometrical shapes and may pollute the contact interaction model. In the contact interaction type problems the resistance of the structure to penetration is increased if the failed elements are not eroded. Vice versa, if they are eroded immediately at the moment of failure in any direction, the simulated resistance to penetration is inadequately low. Therefore the determination of proper value of erosion strain is important for realistic simulation of the impact and penetration behaviour. In this study the ERODS values are selected in conformity with sample simulation results presented in the next section. We used the smallest value of ERODS, the further increase of which makes only very small influence on the residual velocity of the projectile as it perforates the fibre ply.

Certain adjustments of material constants are necessary in the near-to-impact zone, which is presented by the narrow strips model. The idea of making the failure of fibres bundles to start at gaskets lines requires that easy failure of the narrow strips elements in the direction perpendicular to the fibres direction should be prevented. The width and stiffness of the gasket have to be adjusted in such a way that the near zone fibre bundle and neighbouring gaskets junctions treated as *a mezzo-cube* must provide the same homogenized material property values as were obtained by analysing the micro-cube of the fibre ply, Fig. 2. The dimensions of the mezzo-cube are dependent on the width of the narrow strip. In this study we used a simplified way for determining the material constants. The stiffness of the mezzo-cube in the transverse direction, as well as, in shearing is determined by serial connection of the stiffness of the narrow strip and of the polymeric gasket elements. The combined stiffness should provide the same stiffness constants values as obtained from the micro-cube analysis.

The following formulas are employed for obtaining the modified stiffness constants of the narrow strip.

$$\frac{D}{\widehat{E}_b}+\frac{d}{\widehat{E}_g}=\frac{D+d}{\widetilde{E}_b}, \tag{4}$$

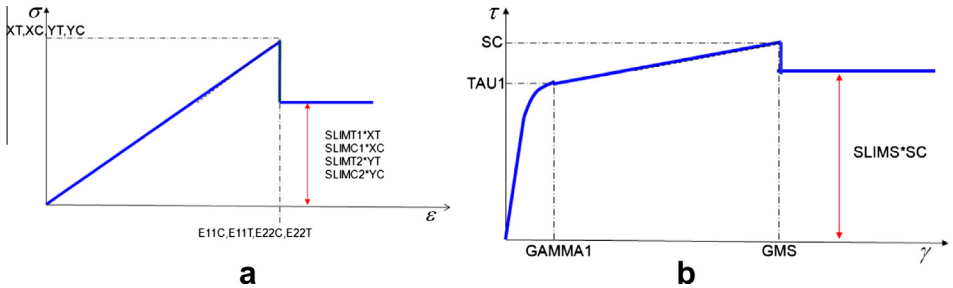


**Fig. 5.** Longitudinal (a) and shear (b) stress–strain-failure models and parameters of NCLCF orthotropic material.

where $D$ is the width of the narrow strip (Fig. 2), $d$ is width of the gasket (Fig. 2), $\widehat{E}_b$ is Young's modulus of the narrow strip to be determined, $\widehat{E}_g$ is Young's modulus of the polymeric gasket, and $\widetilde{E}_b$ is the transverse Young's modulus of the fibre ply determined from the analysis of the micro-cube.

In (4) the left-hand side represents the combined compliance of the narrow strip and the gasket and the right-hand side represents the transverse compliance of the fibre ply of width $D + d$.

The Young's modulus in the transverse direction of the ply is calculated as

$$\widehat{E}_b = \frac{\widetilde{E}_b \widehat{E}_g D}{\widehat{E}_g(D+d) - \widetilde{E}_b d}. \tag{5}$$

Similar calculation is valid for the shear module.

The formula for the modification of the longitudinal Young's module reads as follows:

$$\widehat{E}_a D + \widehat{E}_g d = \widetilde{E}_a (D+d), \tag{6}$$

$$\widehat{E}_a = \frac{\widetilde{E}_a (D+d) - \widehat{E}_g d}{D}. \tag{7}$$

The obtained values are listed in column "Narrow strips" of Table 1. The differences between the stiffness constants values of the orthotropic homogeneous fibre ply model and of the narrow strips elements are quite small at this particular model geometry $D = 1$ mm, $d = 0.001$ mm. However, the differences increase as the width of the gasket is bigger.

### 3.3. Macro-level orthotropic membrane model

Two options of a macro-level model are based on two alternative assumptions that a fibre ply or a fabric sheet are behaving as homogeneous membranes. Further in the text we refer to these options as Macro model 1 and Macro model 2. Numerical examples indicate that such modelling assumptions are much more 'rough' than the narrow strips model. However, the macro-level models are attractive because of significantly lower computational costs. In the problems under consideration the savings of computational resources are achieved due to smaller number of elements taking part in contact interactions. Macro model 1 is obtained straightforwardly from the narrow strips model by presenting the whole fibre ply as the 'farther zone', i.e. without narrow strips refinement. Macro model 2 is obtained by using the layered membrane elements. They are designed to simulate the behaviour of solid multilayer shells by employing a unique integration point through the shell thickness for each individual layer. In this model a layer corresponds to a fibre ply. Each sheet may be constructed layer-by-layer of several plies of different directions. The plies of the multilayer element present the homogeneous solid structure. This means the plies do not work as individual parts. The same NCLCF material model is used for each individual layer. The orientation of the material axes of each layer may be different. The failure, which leads to the stiffness reduction, may take place individually in each layer as limiting stress values are reached. On the contrary, the same value of element erosion strain is used for all the layers, therefore in case of erosion the whole multilayer element is eroded.

There is no ground to choose the values of homogeneous fibre ply mechanical constants other than were used for the farther zone of the narrow strips model. The only parameter to be adjusted individually for each model is the value of the element erosion strain. This is because the element erosions have different mechanical meaning in mezzo and macro models. In the next section we demonstrate that proper choice of the erosion strain may provide a satisfactory agreement between results provided by mezzo and macro models.

### 3.4. Material model of polymeric filling

In our study, the material properties of the polymeric filling are used in several cases. The material is used in the micro-cube model as 3D solid element with the properties listed in Table 1. In the mezzo level model the material is used for shell elements of gasket lines in-between the narrow strips. The value of failure stress of the material is used in tie-break contact description between neighbouring fibre plies of each fabric sheet.

### 3.5. Material model of a bullet

In this study the interactions of deformable 6 mm and 7.62 mm lead bullets against the NCLCF sheets and multilayers has been simulated. The dynamic parameters of the lead material have been investigated by us in earlier publication [5], where we compared computed and experimental shapes of the deformed structure obtained after shooting the lead bullet into the lead plate. The kinematic hardening and the Symonds–Cowper yield stress model were employed. The parameters of the lead material model are listed in Table 2.

## 4. Numerical experiments

### 4.1. Convergence of the narrow strips model

The narrow strips model of the fibre ply has its background in the reality, as the unidirectional ply is formed of parallel slightly twisted bundles of fibres rather than of ideally parallel individual fibres. Nevertheless, there is no ground to assume that the real fibre bundle is something like a thick solid aramid strip. The narrow strips model is based precisely on the assumption of the existence of solid strips. Therefore the model must be convergent as the width of strips is decreased in order to produce results adequate to the reality.

The approach for testing the convergence of the model of the ply of the non-crimped fibres structure has to be clearly defined. A straightforward comparison of nodal displacements of differently refined models cannot be applied in the situations where elements failures and other essential structural changes take place during ballistic impact interactions. Certain integral quantities should be compared rather than nodal displacements and stresses. Our approach was to estimate the time relationships of the bullet velocity obtained by using differently refined models before and after penetration of the ply, and to inspect visually the geometrical shape of the failed zone of the ply for comparison among different models. Unfortunately, we could not investigate experimentally a single ply shot-through as "single plies" are not available. Real sheets of NCLCF materials usually contain not less than 4 orthogonal plies, which cannot be detached from each other without damaging their structure.

The numerical experiments demonstrated the convergence of the narrow strips model as the strip width was halved several times. Strips of width 1 mm, 0.5 mm, 0.25 mm and 0.125 mm were used in the models, the views of the damaged zones of which are presented in Figs. 6a–d. Curves 1–4 in Fig. 6e present the time laws of the velocity of the bullet as it penetrates models shown in Fig. 6a–d. In all cases we set the erosion strain parameter ERODS to value 1.2. The value is large enough in order to eliminate elements not earlier than their failure due to the first kind of failure condition is reached and essential reduction of the stress value in

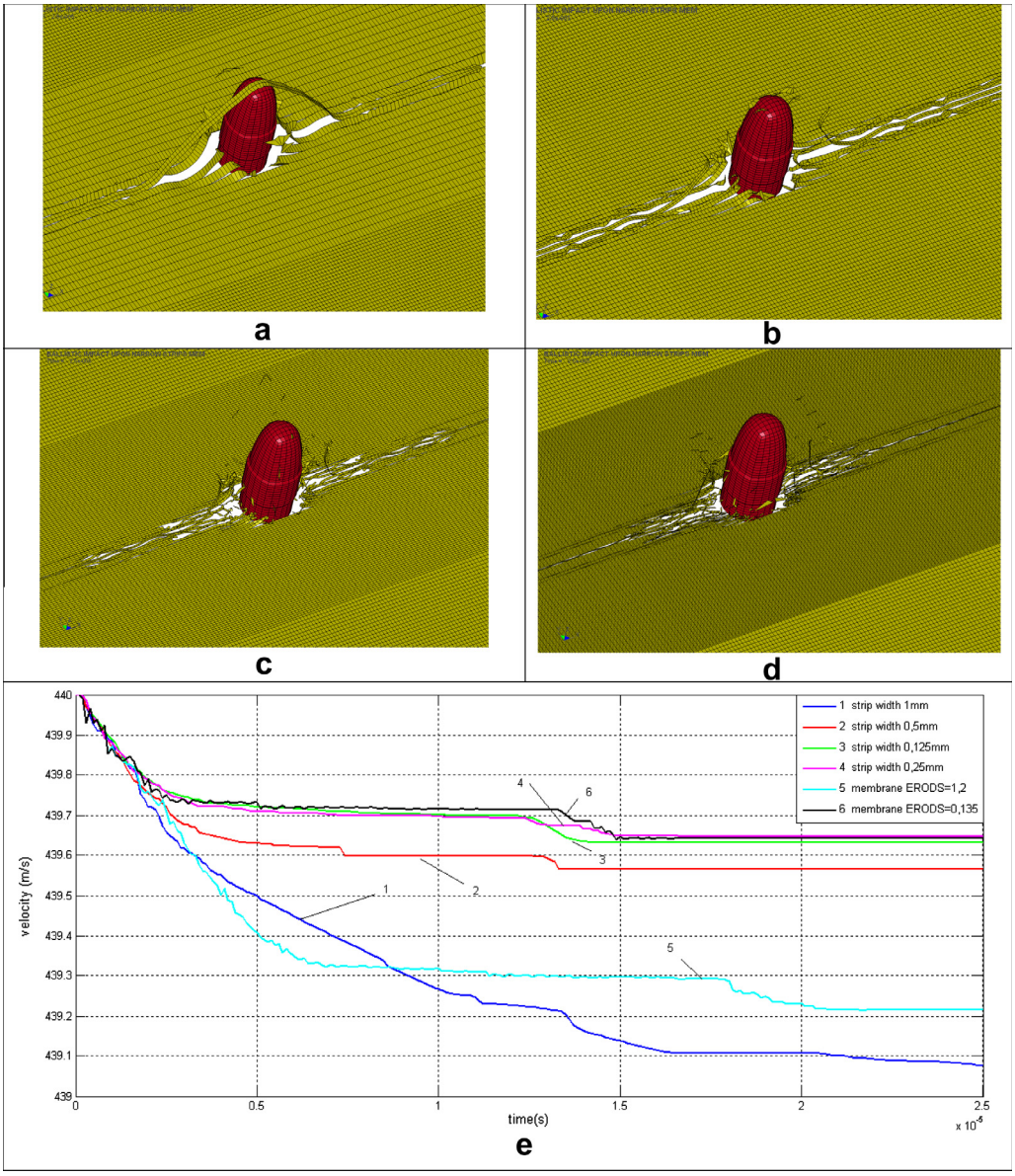


**Fig. 6.** Ballistic penetration of the bullet through a single ply of unidirectional filaments, illustration of the convergence of the narrow strips model. (a–d) – model parts views at time instants 1.36e−5 s, strip width 1 mm (a), 0.5 mm (b), 0,25 mm (c), 0.125 m (d); e – time laws of the bullet velocity (e).

any of characteristic directions takes place. Therefore in this single-ply model ERODS makes practically no influence on the ballistic strength of the ply. On the other hand, the aesthetic view of the pictures Fig. 6a–d are much better as failed elements are removed, and the visual inspection of the geometric shape of the damaged zone is possible. It is difficult to make strict conclusions whether the patterns of failed elements of differently refined models are identical or not. Nevertheless, the observation enables to allege that the shapes of the failed patterns in the models exhibit a tendency to be close to each other as the finite strips are refined.

Several important conclusions may be drawn from this simple numerical experiment. First, the demonstration of the convergence of the finite strips model in terms of the ballistic strength of the ply has been provided. The ballistic strength is the property of the target to reduce the velocity of the projectile or to stop it. It is the main quantitative result expected from the ballistic interaction calculations. This model can be expected to produce reasonable results. If a single ply reacts adequately to impact and penetration by the projectile, the structural model based on a certain number of superimposed plies can be strongly expected to work adequately.

Wider strips tend to artificially increase the ballistic strength of the ply. The continuous orthotropic membrane model employed as the limit case of the finite strips model exhibits the ballistic strength much higher than was obtained by using narrow strips, compare curves 1 and 5, Fig. 6e. In the latter case the ERODS parameter value may be decreased in order to achieve realistic values of the ballistic strength. Smaller ERODS values enable to remove the elements earlier than their stress has been reduced in all directions. Curve 6 presents the bullet velocity time law, where ERODS value was diminished from 1.2 to 0.135. At the same ballistic strength of the ply the shape of the failed zone of the membrane is different from the one obtained by using narrow strips models. However, the similar area of the zone may be obtained by using an appropriate ERODS value.

Properly refined narrow strips model further in this text is regarded as a reference model for evaluation of the performance of rougher models.

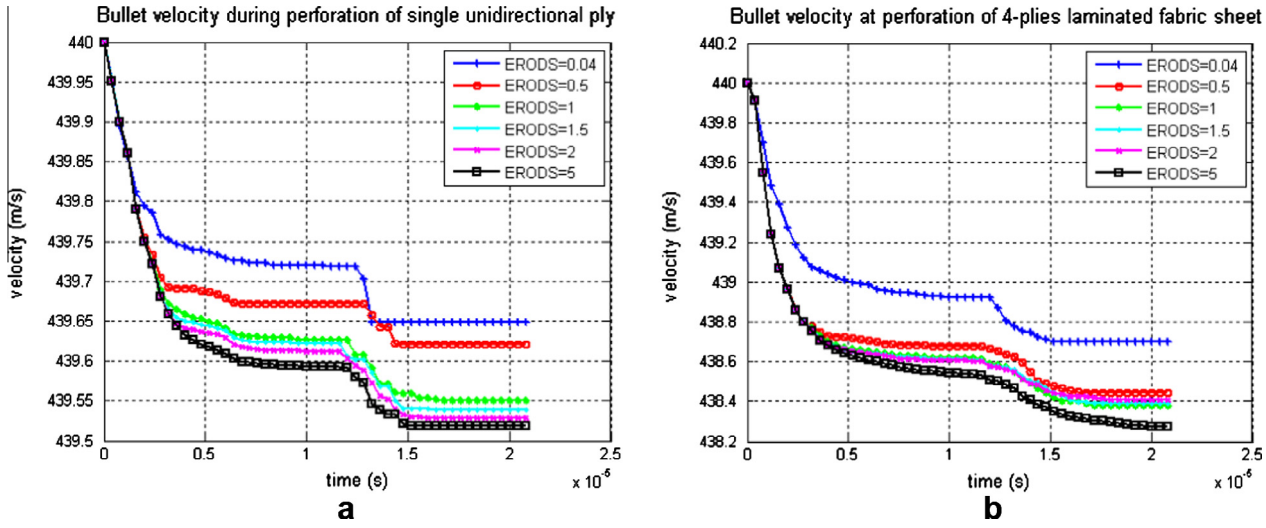


**Fig. 7.** Time laws of the bullet velocity at different values of erosion strain, as the bullet perforates a single ply of unidirectional filaments (a) and 4 plies fabric sheet (b).

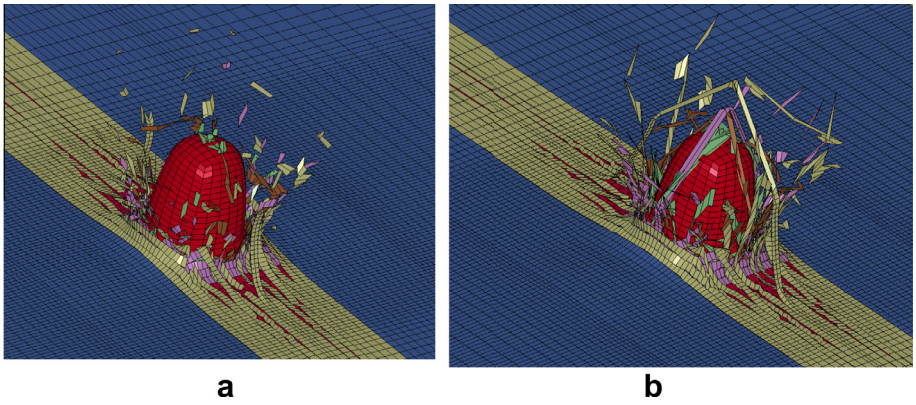


**Fig. 8.** Ballistic perforation of 4-plies sheet at time instant 1.59e−5 s. Element deletion strain values ERODS = 2 (a) ERODS = 5 (b).

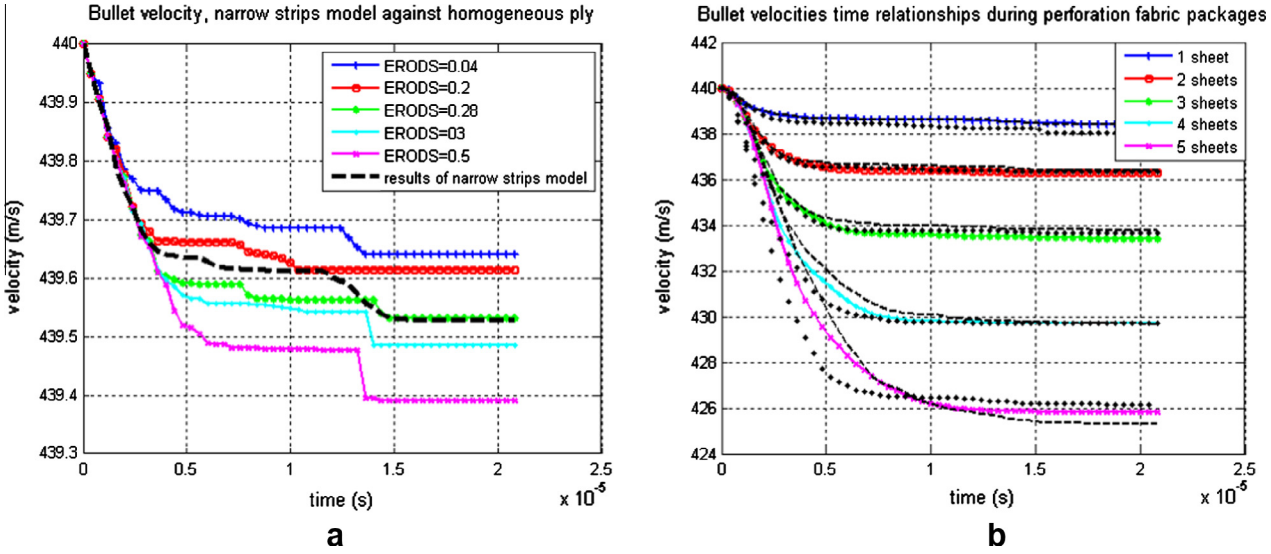


**Fig. 9.** Comparison of the results obtained by using mezzo and macro models: (a) – time laws of bullet velocity at different values of erosion strain, as the bullet perforates the single ply of unidirectional fibres. Dashed line – the reference velocity relationship obtained from the narrow strips model; (b) – time laws of bullet velocity during perforation packages of different numbers of NCLCF sheets; Dashed lines – the velocity of the bullet in Macro model 1 at ERODS = 0.19; Dotted lines – the velocity of the bullet in Macro model 2 at ERODS = 0.135.

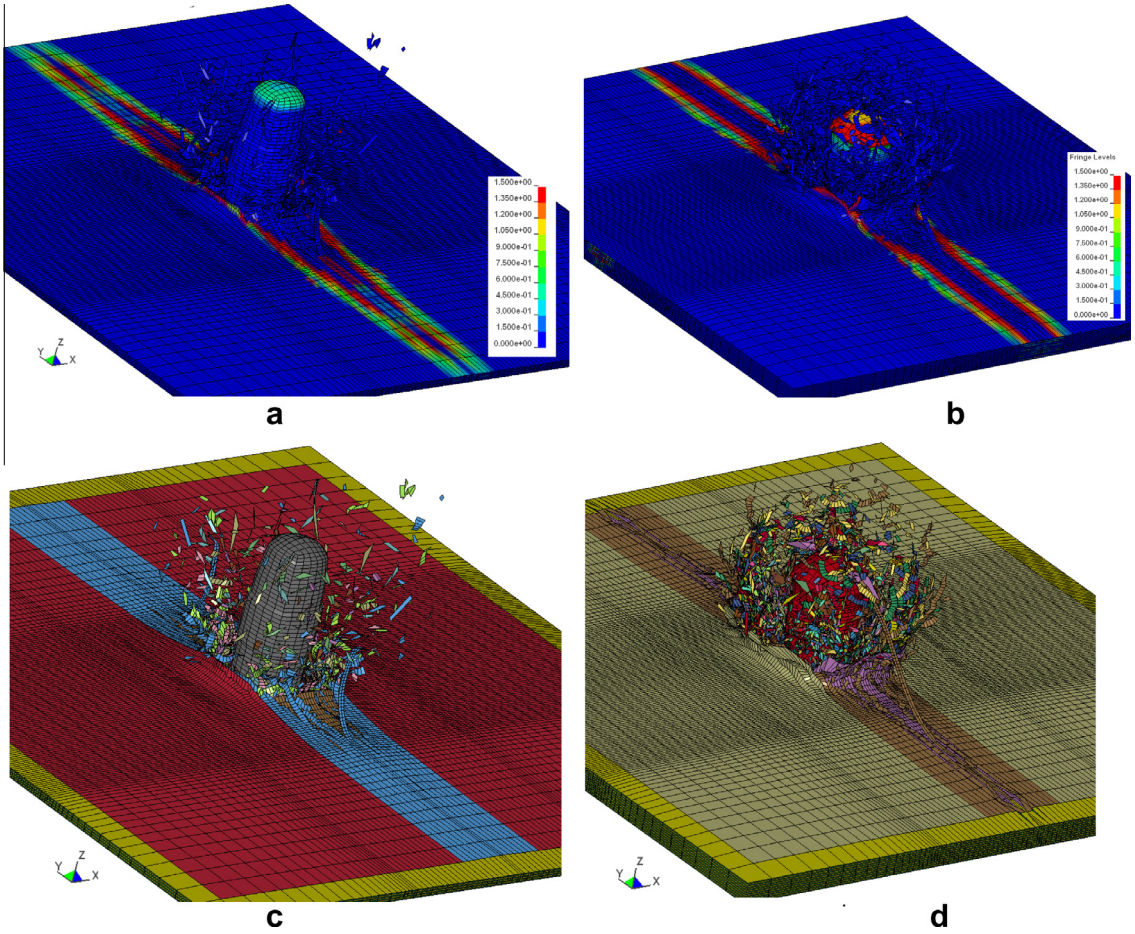


**Fig. 10.** Contours of plastic strain during ballistic penetration of the bullet through 2 fabric sheets (a, c) and 5 fabric sheets packages (b, d) at time instant 3.07e−5 s at initial bullet velocity 440 m/s. Contours of plastic strain (a, b) and the model parts views (c, d).

### *4.2. Influence of the erosion strain value*

ERODS value may be treated as an additional measure in order to control the value of the ballistic strength determined by numerical simulation. In Section 4.1 we referred it to as the second kind of failure condition of the laminated composite fabric material model. An element is deleted from the model as effective strain of the element exceeds ERODS value. If ERODS value is low, the element can be deleted even earlier than it exceeds failure strains along characteristic directions. Such a situation cannot be treated as physically valid. A too high ERODS values failed elements remain in the model all the time of simulation. The question we have to answer is what ERODS value or range of values should applied in order to obtain acceptable results and what tendencies or inadequacies of the model behaviour could be expected if this range of values is violated.

We start at the point that the minimum reasonable value of ERODS is equal to the element stiffness reduction strain E11T or E22T, see Section 3.2. Lower ERODS values will cause deletion of elements which are fully intact yet. For aramid materials this value is approximately 0.04. The time relationship of the bullet velocity during perforation of a single ply of fibres is presented in Fig. 7. Due to early deletion of elements just after they fail along a single longitudinal direction we have the minimum reduction of the bullet velocity after the perforation among all of the investigated cases. As could be expected, the higher ERODS values tend to provide major decrease of the velocity. However, at ERODS > 1 only insignificant changes of the time relationships of the bullet velocity are observed. This can be easily explained as at this range of ERODS values no element is deleted earlier than it fails along all characteristic directions. In this way no artificial strength reduction of the ply takes place, and the resulting bullet velocity is nearly independent of the ERODS value. Therefore all the curves corresponding to values 1, 1.5, 2 and 5 demonstrate acceptable solutions. Obviously the finite strip width must be properly selected as was demonstrated and discussed in Section 4.1.

Nevertheless, we cannot be fully satisfied with the statement that any ERODS value greater than 1 can be freely chosen without influencing the bullet velocity and simulated ballistic strength of the ply. The similar numerical simulation of ballistic perforation of 4 plies NCLCF sheet demonstrated the bullet velocity time relationships as presented in Fig. 7b. The presented curves corresponding to ERODS values from 0.04 to 5 demonstrated an effect, which could not be observed in Fig. 7a. Though curves corresponding to values 1.5 and 2 nearly coincide demonstrating no further influence on ERODS value, the curve corresponding to value 5 indicates further major decrease of the residual bullet velocity. The explanation is that value ERODS = 5 was too big and large number of elements, the stresses of which have been reduced due to the first failure condition resided in the structure for too long time period not only above the surface of the structure but also within interply gaps. The excessive geometrical enlargement of undeleted failed elements is the inherent feature of development of their shape during the time period of analysis. In the mathematical model such elements play the role of artificial obstacles, which are able to reduce the bullet velocity. In reality the particles of failed fibres

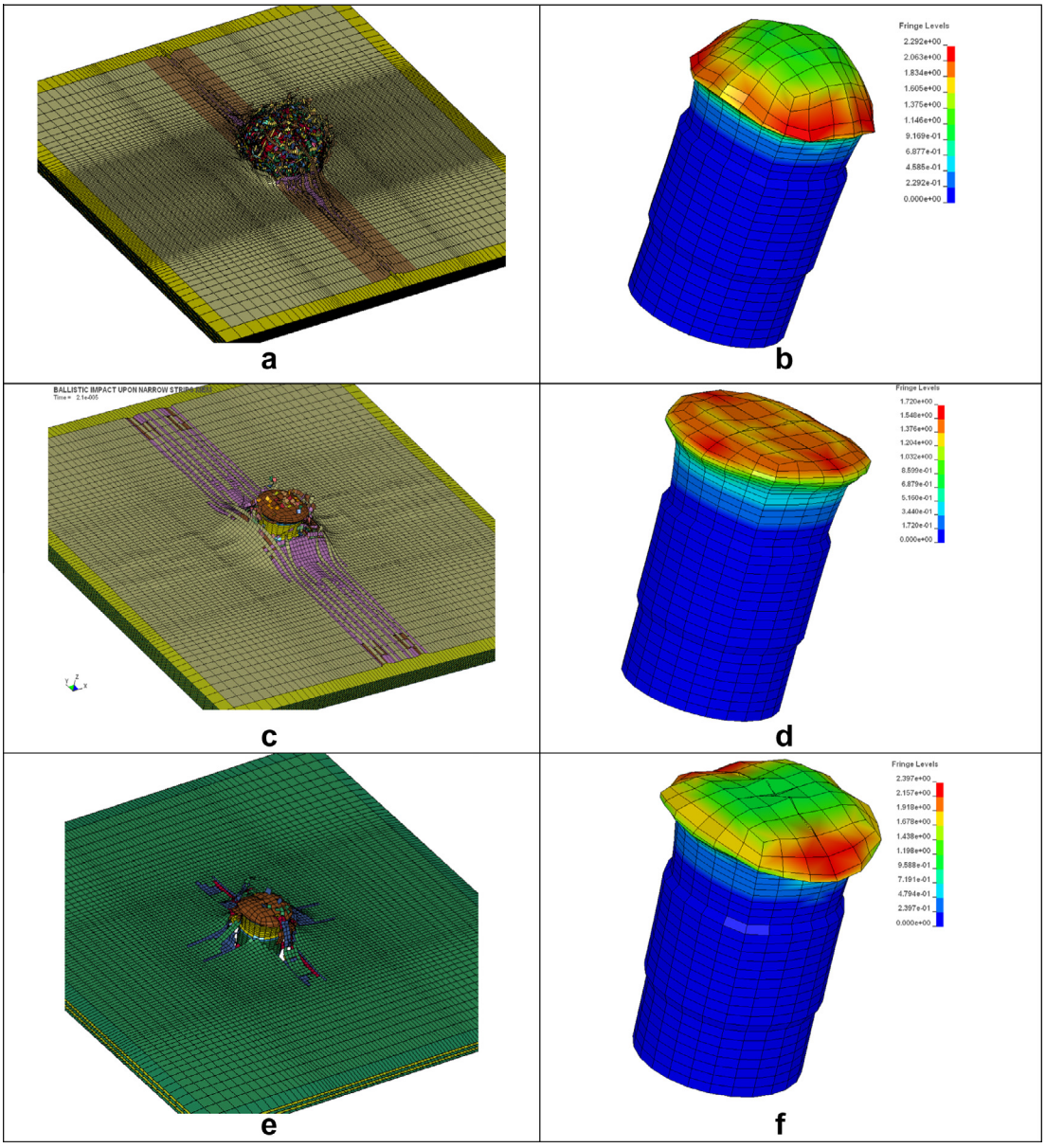


**Fig. 11.** Parts views of the deformed shape of the model at perforation of five sheets NCLCF by using the narrow strips model (a), the Macro model 1 (c) and Macro model 2 (e) at time moment 2.1e−05 s. (b, d, f) – deformed shape and plastic strain contours of the bullet.

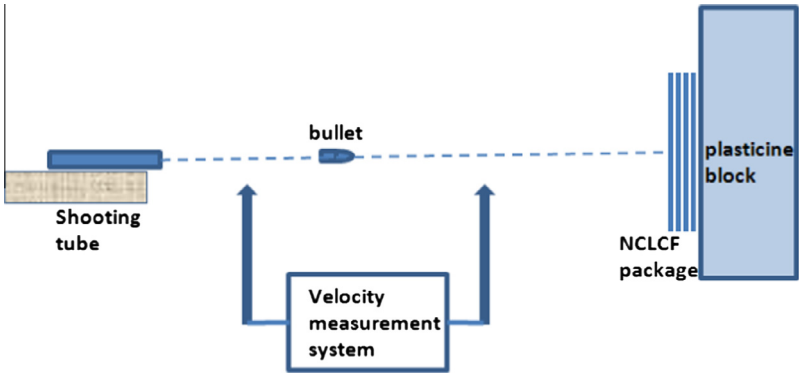


**Fig. 12.** Scheme of the ballistic test of multilayer NCLCF packages.

are much smaller than the elements of the model (recall that elements in the model present fibre bundles rather than individual fibres). Practically they cannot create marked impediments to bullet penetration. The effect of large ERODS values is illustrated by comparing the model parts views during the perforation at time instant 1.59e−5 s obtained at two values ERODS = 2 and ERODS = 5, Fig. 8a and b. At value ERODS = 5 the non-eroded elements obviously tend to acquire unrealistic geometrical dimensions, and the simulated residual bullet velocity begins to decrease with further increase of the ERODS value.

On the base of the above consideration ERODS values 1.2–2 could be recommended for such kind of narrow strips models. Greater values are physically not acceptable.

### 4.3. Bridging the gap between mezzo and macro-level models

We demonstrated that the mezzo level model developed in this work is an operative one. It is able to present the most important mechanical features of the analyzed system. The model is based on the narrow strips structure and therefore to a certain extent not convenient for everyday engineering computations due to its complexity. A macro-level model, which presents the NCLCF sheet structure as continuous orthotropic membrane would be much more attractive tool for engineering computation. Here we investigate about the possibility to present the NCLCF ballistic interaction model at macro-level. The model should work with sufficient adequacy to the reality at small and large strains, as well as, at penetration failure.

From previous analysis we know that proper adjustment of influence of two different kinds of failure may provide coherent ballistic strength values obtained by using mezzo and macro models. In the numerical experiment described in Section 4.1 we achieved it easily by adjusting the ERODS value of the macro model, which caused slightly premature deletion of the failed elements and in this way reduced the computed ballistic strength of the membrane model. The impact interaction behaviour was obtained similar to the behaviour of the softer structure based on finite strips. However, this is not enough for the two models to be mutually equivalent. The same adjusted ERODS value must be suitable for problems treating ballistic interaction of packages containing arbitrary number of NCLCF plies and sheets. Two important points should be mentioned as the number of NCLCF sheets is increased. Huge numbers of elements fail during simulation of the penetration through the sheets package. In continuous membrane models the apropos deletion of elements due to properly selected ERODS value is crucial for obtaining the reasonable estimation of the ballistic strength. The other point is that the bullet is markedly deformed as it hits thick packages. The effective area of interaction increases considerably. Dependent on the number of sheets impacted, the change of the geometric form of the bullet may vary from slight flattening of the initially rounded bullet nose to acquiring the mushroom or even pancake shape. The phenomena of deformation of the bullet nose and failure of the sheet package are closely interrelated. By adjusting the ERODS value we also change the effective hardness of the sheet surface, which directly influences the bullet nose deformation and thus the reduction of the bullet velocity due to different area of interaction. At the first impression it seems as hardly possible to ensure at least approximate coherence of the mezzo and macro models in all above mentioned aspects by means of single proper ERODS value. However, the results presented in Fig. 9 demonstrate that in this problem it works.

Fig. 9a presents the time laws of bullet velocity at different values of erosion strain as the bullet perforates a single ply of unidirectional filaments presented by Macro model 1. The change of the narrow strips model to Macro model 1 is rather straightforward, as the material model of the membrane model of the ply is essentially the same as of the farther zone of the narrow strips model. However, the failure of continuous membrane sheet due to transverse and shear strain might take place in a different way than in the narrow strips model. The dashed line presents the reference time relationship obtained by using the mezzo level narrow strips model and should be regarded as the reference curve. By looking for the best fit between the curves obtained by means of the two models from this numerical experiment it could be estimated that ERODS = 0.2 is a reasonable choice. The value was corrected to 0.19 by investigation of penetration through the fabric packages containing different number of sheets. Similar numerical investigation was carried out on Macro model 2 and ERODS = 0.135 was obtained.

In Fig. 9b the bullet velocity time relationships during perforation of 1–5 fabric sheets packages are presented, where each sheet

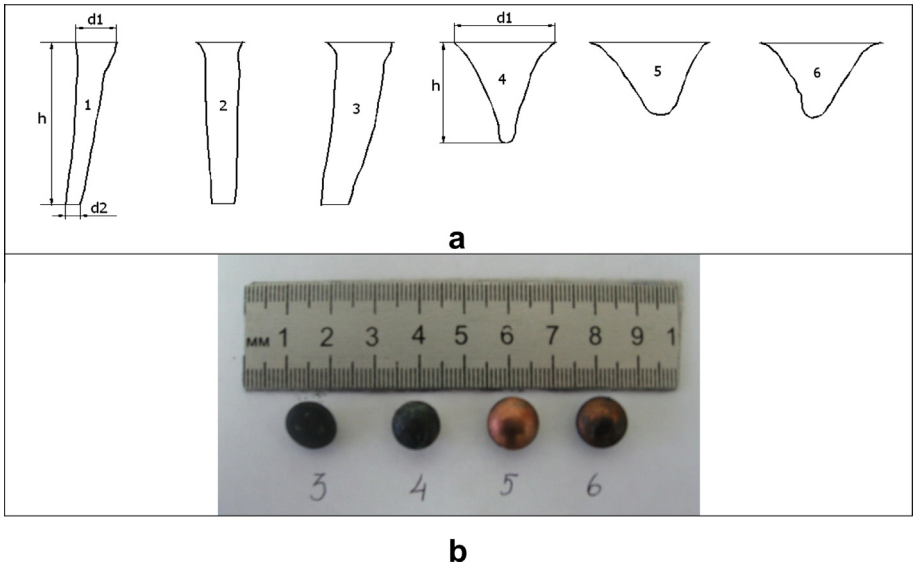


**Fig. 13.** Sockets in the plasticine after ~310 m/s ballistic tests on 1–6 sheets layers NCLCF packages (a) and deformed noses of bullets after the impact on packages of 3, 4, 5 and 6 sheets (b).

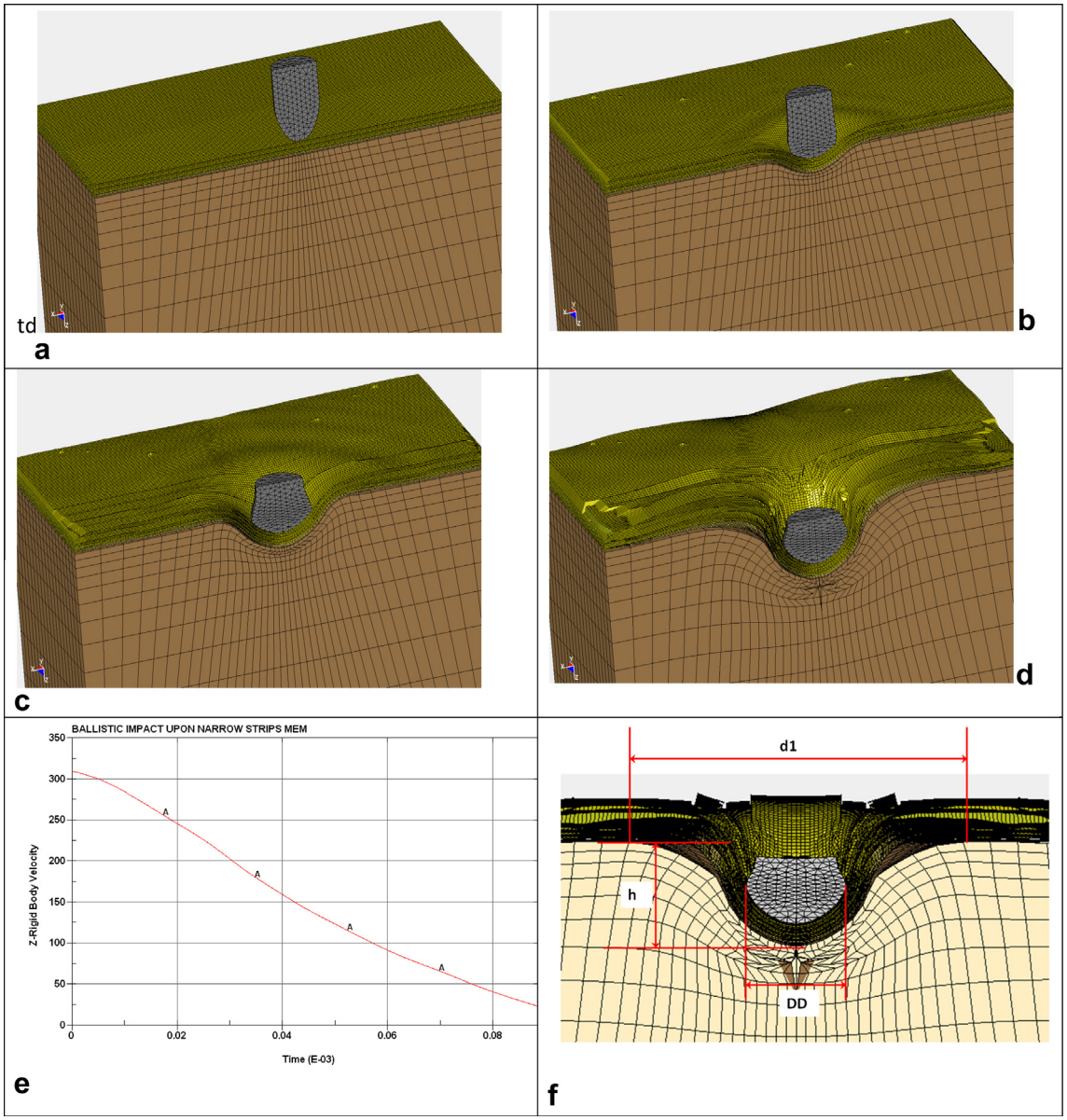


**Fig. 14.** Simulated ballistic test on six sheets NCLCF package, view before the impact (a), at $1.85 \times 10^{-5}$ s (b), $3.3 \times 10^{-5}$ s (c), $8.86 \times 10^{-5}$ s (d), time relationship of bullet velocity (e) and characteristic measurements of the after impact geometrical configuration for comparison of simulated and experimental results (f).

consists of 4 unidirectional fibre plies. It may be observed that the selected ERODS values ensure very similar bullet velocity relationships by using narrow strips model at ERODS = 2, Macro model 1 based on membrane models of plies (see Section 3.2) at ERODS = 0.19 and the Macro model 2 based on membrane models of sheets at ERODS = 0.135. The same ERODS values worked satisfactorily at different numbers of sheets in all investigated cases.

The deformed geometry of the model parts and the contours of the plastic strain are presented in Fig. 10 in the cases of 2 and 5 sheets fabric packages perforation. In accordance with the material models used in mezzo-level model, the plastic strains take place in the bullet and in the gaskets in-between the narrow strips of the near-to impact zone. This reflects the real situation in the plies, where the plastic behaviour takes place due to transverse and shear deformations of the polymeric filling.

Next we make an effort to adjust the Macro model 2 erosion strain value on the base of comparison of the results against the reference results. For Macro model 2 the erosion strain value ERODS = 0.135 is obtained. The check of the obtained value is presented in Fig. 9a, where dotted lines correspond to numbers 1–5 of fabric sheets in the package. The views of the deformed structures of the three models at time moment 2.1e−05 s are presented in Fig. 11a–e.

Though the three models provide good mutual agreement in terms of the residual bullet velocity, the macro models give higher plastic strains in the bullet nose. Generally, the homogeneous membrane models are "harder", therefore they cannot completely substitute the mezzo level narrow strips model. However, the membrane models are much more efficient from the computational point of view and may be applied for rougher approximations of ballistic resistance of fabric packages. The narrow strips might be efficiently employed for the adjustment of certain mechanical parameters of the macro model.

### 4.4. Comparison against ballistic test measurements

Ballistic tests with 7.62 mm lead core 4.6 g bullets have been performed on NCLCF packages of 4 plies Twaron GF4 aramid

**Table 3**
Results of ballistic tests and simulations at average bullet velocity 310 m/s.

| Number of sheets | Bullet velocity (m/s) | h (mm) | | d1 (mm) | | DD (mm) | | d2 (mm) | Number of penetrated sheets | |
|---|---|---|---|---|---|---|---|---|---|---|
| | | Experiment | Simulation | Experiment | Simulation | Experiment | Simulation | Experiment | Experiment | Simulation |
| 1 | 329 | – | – | 14.4 | 13 | 7.7 | 7.7 | 6.1 | 1 | 1 |
| 2 | 300 | – | – | 17.5 | 16 | 7.7 | 7.9 | 10.1 | 2 | 2 |
| 3 | 310 | – | – | 24.9 | 20 | 8 | 8.2 | 11.7 | 3 | 3 |
| 4 | 305 | 38.4 | 26 | 39.5 | 32 | 8.5 | 8.8 | – | 1 | 2 |
| 5 | 317 | 28.3 | 21 | 43.7 | 36 | 9.5 | 9.6 | – | 0 | 1 |
| 6 | 298 | 28.3 | 20 | 46.1 | 38 | 11 | 10.8 | – | 0 | 0 |

h – Depth of the socket.
d1 – Diameter of the socket at bullet entrance plane.
d2 – Diameter of the socket at bullet exit plane.
DD – Diameter of the deformed bullet.

sheets. The principal scheme of the ballistic test is presented in Fig. 12. The experimental equipment consists of the shooting tube, bullet velocity measurement system and the NCLCF package attached against the 5 cm thick plasticine block. The soft block is employed in order to imitate the human body protected by means of the package. The block itself exhibits no essential resistance to the bullet penetration. Covered with the NCLCF package it enables to create realistic working conditions of the package. On the other hand, the presence of the block ensures the proper positioning of the package during the ballistic test. After the test the size of the socket in the plasticine at the impact zone is measured in order to evaluate the possible injury. In simulations it was assumed to be a material much softer than the material of the bullet of mass density 1570 kg/m$^3$. The edges of NCLCF sheets in reality should be considered as free. However, the dimensions of the real sheet are much bigger than the modelled part of the sheet. Therefore in the model the edges are fixed by means of soft elastic supports.

Fig. 13 presents pictures of the socket profiles and of deformed bullets obtained after shooting through 1–6 sheets NCLCF packages. Fig. 14 presents the results of computer simulation of the shot through 6 sheets. Simulation and experimental quantities to be compared are the depth and diameters of the sockets and number of sheets shot-through during ballistic tests. From simulations results we could not establish the socket diameter at exit (bottom of the plasticine block). Due to very large distortions of the element mesh it appeared problematic to continue the simulation until full penetration of the block. On the other hand, practically it was enough to fix the fact that the package could be perforated by the bullet.

The simulated and experimental values can be compared in corresponding columns of Table 3. The general correspondence between the results could be considered as satisfactory regarding the complexity of the system and aggregated character of measured data. The change of the shape of the bullet is very similar in experiments, as well as, in simulations. The number of perforated sheets of the package also was estimated satisfactorily. The sockets, which remain in the plasticine, in simulations were obtained of about 20–30% of smaller dimensions than in the experiment. Two reasons could be suggested for the explanation. First, the material properties of the plasticine model were not investigated thoroughly. The form and depth of the socket are dependent on the properties of the plasticine material. Second, it is known that experimental values of the socket dimensions may become bigger than the deflection of the package due to another effects the mechanisms of which are not described in the investigated model.

Though the compared integral quantities cannot be considered as direct evidence of validity of the models, they indicate that the developed models may provide reasonable and similar to reality results.

## 5. Conclusion

In computational models of higher complexity certain failure parameters values are inevitably selected without exact measurements and without knowing the values in advance. The natural requirement is that the influence on the model behaviour should not contradict with the real behaviour of the object. Suchlike are the parameters of filling materials, which perform their function by keeping the internal structure of laminated composite fabric sheets structure intact before the impact rather than working for ballistic strength. Usually soft filling materials fail at the very beginning of the impact interaction. Often we use the material constants, which may be appropriate for materials similar to the ones used in this particular composite fabric. In our calculations we used the elastic–plastic material model of low density polyethylene as a representative material of polymeric filling.

The main result of this investigation is a more or less successful 'architectural' solution of the family of three models. The main idea is based on model reduction, where comparatively rough yet operative and computationally efficient macro-scale models are synthesized by employing the results of investigation of micro and mezzo scale models of much higher refinement and complexity. The narrow strips model and macro models 1 and 2 described in this work were composed by following the logic of decreasing minuteness, where some behavioural details of the refined model were integrally assessed within the rougher model. Therefore not only formal, however also physical and computational compatibility among the models takes place.

We did not perform experimental comparisons, which could directly serve as model validation experiments. Nevertheless, certain indirect comparisons based on final configurations of the ballistic interaction have been made, which indicate that the simulation results are at least in close resemblance to the real processes that take place during ballistic tests on NCLCF packages. On the other hand, it is very difficult to experimentally evaluate the details of the impact interaction process on highly flexible target structures and easily deformable projectiles in the range of ballistic velocities and to obtain clear and undoubted validation evidences. Probably, it is the topic of another research. As an example, the socket in the plasticine target sometimes may be deeper than the real penetration of the bullet because of wave dynamics phenomena in the vicinity of the impact. Uncertainties are introduced because of loosely defined boundary conditions at the edges of fabric sheets.

The orthotropic material parameters have been established by investigating the physical behaviour of the ply at the micro-level. We considered them as true in mezzo and macro-level models. However, the interactions in the investigated system are so complex that parameters of the model inevitably require empirical

adjustment in order to represent the reality in an adequate way. This is generally known in many complex simulation problems in ballistics, automotive crash and other fields. Different interaction velocities, different structures of the projectile, different model refinement levels may require certain adjustments of the viscosity, plasticity, hardening and failure parameters values in order to improve the adequacy of simulation results. This research demonstrated that the element erosion strain parameter offered by LSDYNA software for shell elements within certain limits may be successfully used as a simple and efficient 'handle' for model adjustments. The established rather simple mutual relation by means of proper selection of erosion strain parameter provides evidence of physical compatibility among the three different models.

The important issue is a discussion on the versatility of obtained results. The upper limit of impact velocities very probably should be regarded as ~300–450 m/s, which is typical for pistol bullets. It is assumed that in this range of velocities the material models based on orthotropic elasto-plasticity may be employed in the models. The aramid materials in this velocity range fail immediately after the elastic deformation stage. The impact wave propagation phenomena are important during the interaction as the value of the bullet velocity is comparable with the wave propagation speed in the target NCLCF package. Areas of sheets at least several times bigger than the diameter of the bullet are involved into interaction. At higher velocities equation-of state models would be preferable and impact processes take place only in the nearest vicinity of the impact. Consequently, the architecture of the models should be different.

It should be admitted that the obtained results cannot be transferred to plies and sheets of different composition without any analysis. We think that the ballistic behaviour of plies and sheets of another composition should be investigated a priori in order to be sure that the models of sheets work properly. On the base of verified models of the sheets complex package structures can be simulated. Very probably the established model parameters are valid only for certain element size ranges. The parameters should be re-established if there is a need to markedly change the refinement of the model.

This study was devoted mostly to model architecture and computational issues. Many more details regarding the values of mechanical constants and their relationships against the strain rate, models and effects of friction interactions should be addressed in future investigations. Though certain information about dynamic properties of aramid materials is available, in this study we employed only the basic properties and mechanical laws, which are essential for demonstrating the validity of the proposed structural composition of the models.

## Acknowledgement

The research has been sponsored by the Lithuanian Science Council, Agreement Number MIP-31/2011.

## References

[1] Pavliotis AG, Stuart AM. Multiscale methods averaging and homogenization. Springer; 2008. 307 p..
[2] Efendiev Y, Hou TY. Multiscale finite element methods. Springer; 2009. 234 p..
[3] Tserpes KI, Labeas GN. Mesomechanical analysis of non-crimp fabric composite structural parts. Compos Struct 2009;87:358–69.
[4] Gao XL, Li K, Mall S. A mechanics-of-materials model for predicting Youngs modulus of damaged woven fabric composites. Int J Solids Struct 2003;40:981–99.
[5] Barauskas R, Vilkauskas A. Modeling of bullet interaction against the life protection textile. In: Proceedings of the Nordic LS-DYNA users' conference, 2002, proceedings on CDROM.
[6] Barauskas R, Abraitienė A. Computational analysis of impact of a bullet against the multilayer fabrics in LSDYNA. Int J Impact Eng 2007;34(7):1286–305.
[7] Tan VBC, Ching TW. Computational simulation of fabric armour subjected to ballistic impacts. Int J Impact Eng 2006;32:1737–51.
[8] Lim CT, Shim VPW, Ng YH. Finite-element modeling of the ballistic impact of fabric armor. Int J Impact Eng 2003;28:13–31.
[9] Duana Y, Keefeb M, Bogetti TA, Cheeseman BA. Modeling friction effects on the ballistic impact behaviour of single-ply high-strength fabric. Int J Impact Eng 2005;31:996–1012.
[10] Zohdi TI, Powell D. Multiscale construction and large-scale simulation of structural fabric undergoing ballistic impact. Comput Methods Appl Mech Eng 2006;195:94–109.
[11] Nilakantan G, Keefe M, Bogetti TA, Gillespie JW. Multiscale modeling of the impact of textile fabrics based on hybrid element analysis. Int J Impact Eng 2010;37:1056–71.
[12] Nilakantan G, Keefe M, Bogetti TA, Adkinson R, Gillespie JW. On the finite element analysis of woven fabric impact using multiscale modeling techniques. Int J Solids Struct 2010;47:2300–15.
[13] Wang Y, Miao Y, Swenson D, Cheeseman BA, Yen CF, LaMattina B. Digital element approach for simulating impact and penetration of textiles. Int J Impact Eng 2010;37:552–60.
[14] LS-DYNA Theory Manual. Livermore software technology corporation; March 2006, 680p.